Low-temperature behavior of krypton monolayers on graphite

Neil D. Shrimpton and Béla Joós
Ottawa-Carleton Institute for Physics, University of Ottawa Campus, Ottawa, Ontario, Canada K1N 6N5

Birger Bergersen
Department of Physics, University of British Columbia, Vancouver, British Columbia, Canada V6T 2A6
(Received 9 February 1988)

A calculation is performed for the low-temperature free energies of defect-free incommensurate monolayers of krypton on graphite. The calculation uses realistic potentials to describe the interactions between the atoms in the system, and takes into account the dynamic nature of the monolayer. The anharmonic nature of the interaction potential between adsorbed atoms causes the low-temperature behavior of the incommensurate monolayer to deviate from that predicted by harmonic calculations. The zero-point energy of the monolayer is significant, and reduces the critical value of the substrate corrugation to 7.0 K if the monolayer is to have a commensurate phase at low temperatures. Also, the zero-point energy cannot be neglected if the variation in the equilibrium misfit of the monolayer with chemical potential is to match that found by experiment. The $\frac{1}{3}$ exponent of the misfit variation is found to be merely a consequence of the fact that the monolayer crosses over from having a domain-wall network to being weakly modulated over the range of misfit values considered by experiment. The value of the exponent is therefore not a universal value: Other similar systems may exhibit different exponents. The entropy contribution to the free energy is found to be small; the interactions between the domain walls, though weak, are sufficient to reduce the entropy of the domain-wall breathing mode. The free energy therefore does not vary significantly as the temperature of the system is increased from zero.

I. INTRODUCTION

In the physics of two-dimensional systems, the krypton monolayer on graphite is probably the best system to illustrate the unique phenomena that can be observed in a physisorbed monolayer.[1,2] This system exhibits a very stable commensurate (C) phase which is extensively used to characterize graphite substrates.[3] The commensurate-incommensurate (C-IC) transition is well defined and has been closely analyzed.[4–12] There is strong evidence for the existence of domain walls in the incommensurate (IC) phase. Several different melting transitions have been identified:[4] These transitions are well predicted by Potts-model calculations.[13] However, despite the simplicity of the system, there is still, after many experimental studies, an incomplete picture of the microscopic nature of the IC phase.

Krypton is a rare-gas atom. The graphite surface forms a honeycomb array of adsorption sites. The interactions between krypton atoms and between the krypton and the graphite surface are all basically of the van der Waals type.[14,15] The adsorption energy of krypton onto graphite is about 1800 K. The equilibrium separation preferred by the krypton atoms is 4.03 Å. This is somewhat smaller than the spacing of 4.26 Å, the lattice parameter for the nearest triangular array of adsorption sites, which is the $(\sqrt{3}\times\sqrt{3})$ C configuration. (4.26 Å $=\sqrt{3}\times 2.46$ Å, the distance between adsorption sites.) In the C phase the krypton monolayer is therefore slightly expanded. As more atoms are deposited on the surface, a transition occurs to an IC phase of higher density. The IC phase consists of commensurate (or registered) regions separated by a regular honeycomb network of walls of higher density.[16–18] A typical incommensurate configuration is shown in Fig. 1. The difference between the averaged krypton spacing of the IC phase and the C phase, called the misfit ε, is known to vary as the $\frac{1}{3}$ power of the chemical potential once the monolayer becomes incommensurate.[8–10] With increased density, the IC phase is also observed to undergo a transition from being aligned with the substrate to being rotated with respect to the substrate.[9,10,12]

In this paper, with the use of realistic potentials, we calculate the free energies of IC configurations for varying misfits and angles of rotation. We are particularly interested in assessing the validity of Shiba's harmonic theory[19,20] for the IC phase and in determining the importance of the contributions of the zero-point energy and the entropy term. As we shall show in Sec. IV A, the inclusion of cubic terms in the interatomic interactions introduces an important new feature into Shiba's theory of orientational epitaxy.[20] The zero-point energy is used in Sec. IV A to calculate a new value for the critical parameter V_g that measures the strength of the rare-gas–substrate interaction. In Sec. IV C, results for the entropy contribution to the free energy reveal that for a larger interval of misfit than it is generally believed the domain-wall interaction is strong. The following section lays down the formalism for this work, while Sec. III describes the calculation.

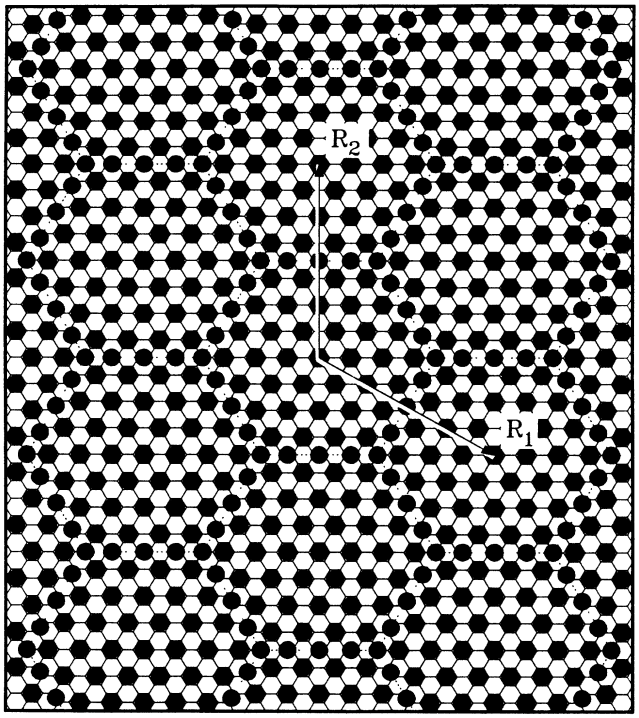

FIG. 1. Typical positions of the adatoms for an incommensurate monolayer with hexagonal periodicity, the vectors $\mathbf{R}_1$ and $\mathbf{R}_2$ are primitive vectors of the superlattice. This is a stylized picture and does not represent a minimum-energy configuration.

II. FORMALISM

The behavior of the monolayer must be considered in the context of the total system of krypton vapor, graphite substrate, and condensed krypton film. The equilibrium configuration is the configuration that minimizes the total free energy of this system. An exact calculation for the total free energy which considers all aspects of the system simultaneously is not practical. However, approximations can be made which separate the free energy into several independent components to reduce the complexity of the problem. This separation has been considered by Villain and Gordon.[21]

The general system is taken to be a sealed chamber of volume V containing N_T krypton atoms and a graphite substrate. The temperature of the system is maintained at T. Under appropriate conditions the krypton will condense onto the substrate to form a solid monolayer. The chamber is assumed to be sufficiently large that the number of condensed atoms, N, is insignificant compared to the total number of atoms, N_T, in the chamber. The equilibrium state will then be the state that minimizes the free energy Λ_c,

$$\Lambda_c = F_c - \mu N \ , \tag{1}$$

where F_c is the Helmholtz free energy of the condensed phase, and μ is the chemical potential of the krypton vapor. The study can therefore be restricted to an examination of the condensed system. The effect of the vapor on the total system is provided by the chemical potential μ which is treated as a parameter.

The energy of the condensed system will involve both potential and kinetic energies. Because the components of the system are quite massive, the dynamic aspects of the condensed phase are, at low temperatures, expected to provide only minor corrections to the information obtained from calculations of the static properties. The free energy of the condensed system can thus be separated into a potential-energy term and a term which depends on the dynamics of the system.

The potential energy of the condensed system is divided into two parts. The first part is the potential energy of the bare substrate; the second part is the energy change when krypton is adsorbed onto the surface. The calculation can be restricted to consider only the latter part because constant terms have no impact on the equilibrium configuration.

A given adsorbed atom (adatom) will be influenced by interactions with neighboring krypton atoms and an interaction with the substrate. The interaction between krypton atoms can be described in terms of a pair potential; the form of the potential used in this calculation is the bulk potential of Aziz[22] modified by the substrate screening as determined by Rauber *et al.*[23] from the theory of McLachlan.[24] Additional influences on the adatom-pair interactions have been discussed in detail by Bruch[15] with the conclusion that they do not have an impact on the configuration of the monolayer.

The substrate interaction, which involves the attraction between substrate carbon atoms and the adsorbed krypton is, however, not as easily described. The charge distribution within the substrate, due to chemical bonding between carbon atoms, complicates the interaction to the extent that it has not yet been modeled reliably. Because of this, a parametrized form of the substrate potential that reflects the symmetry of the substrate is used in the calculation. The substrate potential has the form

$$V(\mathbf{r},z) = V_a(z) - \sum_{\mathbf{g}} V_{\mathbf{g}}(z) e^{i\mathbf{g}\cdot\mathbf{r}} \ , \tag{2}$$

where z is the height of the krypton atom above the substrate and $\mathbf{r}$ is a vector confined to the plane of the substrate with origin at an adsorption site. The summation proceeds over all reciprocal-lattice vectors $\mathbf{g}$ of the substrate.

The dominant term in (2), $V_a(z)$, is the surface average of the potential energy $V(\mathbf{r},z)$. The remaining terms in (2) provide the lateral variation of the substrate potential. As shown by Steele,[14] the lateral variation in the substrate potential influences the adsorbed atoms in two ways: First, the substrate can exert a lateral force on the adatoms, and second, the height z at which each atom sits varies as a function of its lateral position $\mathbf{r}$. For the commensurate monolayer each atom sits above an equivalent site on the substrate and the monolayer is planar. For incommensurate monolayers, however, the adatoms are not all situated at equivalent sites of the substrate and the monolayer is not planar.

Gooding *et al.*[17] have considered the height variation

of the adatoms in the monolayer. They found that because the positions of the adatoms $(\mathbf{r},z)$ are smoothly modulated, the difference in height between an adatom and its neighbors is negligible. The interactions between the adatoms can therefore be calculated as though the monolayer was planar; the heights of the adatoms are dependent only on the substrate interaction. An adatom with a lateral position $\mathbf{r}$ will have a height $z(\mathbf{r})$ at which the substrate interaction is minimized. This minimum-energy distance $z(\mathbf{r})$ defines a surface on which the monolayer lies.

The substrate interaction felt by the krypton atoms which are confined to the surface $z(\mathbf{r})$ can be described by a potential $V(\mathbf{r})$ having a form, similar to (2), that depends only on the lateral position of the adatom. The variation of the substrate potential is so smooth on this surface, however, that summation over reciprocal-lattice vectors can be truncated after the first shell.[14] This leads to a simplified form

$$V(\mathbf{r})=V_0+V_g\sum_{\mathbf{g}}(1-e^{i\mathbf{g}\cdot\mathbf{r}}) , \tag{3}$$

where the summation involves only the first shell reciprocal-lattice vectors. V_g is a parameter, known as the substrate corrugation, which provides the lateral variation in the substrate interaction. Because of the symmetry of the interaction, V_g is a constant that has been factored from the summation.

With a pair potential Φ, which describes the interaction between krypton atoms in the monolayer, and the substrate potential V, which gives the interaction between a krypton atom and the substrate, the potential energy of the monolayer can be calculated. As mentioned above, the height variation in the minimal energy surface $z(\mathbf{r})$ is so slight that the pair interactions Φ between adatoms in the monolayer can be calculated as though the monolayer was planar. The energy of the monolayer therefore is

$$E=\tfrac{1}{2}\sum_{\mathbf{r},\mathbf{r}'}\Phi(\mathbf{r}-\mathbf{r}')+\sum_{\mathbf{r}}V(\mathbf{r}) , \tag{4}$$

where $\mathbf{r}$ and $\mathbf{r}'$ are the lateral positions of the adatoms in the monolayer and the first summation excludes the possibility that both positions coincide.

The potential energy is minimized for configurations of the monolayer in which the positions of the adatoms satisfy the condition

$$0=\sum_{\mathbf{r}'}\nabla\Phi(\mathbf{r}-\mathbf{r}')+\nabla V(\mathbf{r}) . \tag{5}$$

As before, the summation excludes the possibility of coincidence. Equation (5) reflects the fact that the static forces felt by the adatoms are zero when the positions of the adatoms minimize the potential energy.

Because of the interplay of the adatom-pair interactions and the substrate interaction, the atoms will not form a triangular lattice when the monolayer is incommensurate with the substrate. However, the atoms in the monolayer always maintain a hexagonal packing with positions $\mathbf{r}$ that have slight displacements $\mathbf{u}$ from a triangular lattice of vectors $\mathbf{R}$,

$$\mathbf{r}=\mathbf{R}+\mathbf{u}(\mathbf{R}) . \tag{6}$$

The primitive lattice vectors, $\mathbf{d}_1$ and $\mathbf{d}_2$, which generate the vectors $\mathbf{R}$, have lengths determined by the averaged spacing of the adatoms in the monolayer. If the primitive vectors of the commensurate phase are defined to be $\mathbf{D}_1$ and $\mathbf{D}_2$, the experimentally measured quantities of misfit ε and orientation θ are related to these primitive vectors by

$$\varepsilon=\left[1-\frac{|\mathbf{d}_1|}{|\mathbf{D}_1|}\right] , \tag{7}$$

θ being the angle between the two vectors $\mathbf{d}_1$ and $\mathbf{D}_1$. These quantities are also related to the size and arrangement of the domain network. Specifically, the length of the vectors $\mathbf{R}_1$ and $\mathbf{R}_2$ in Fig. 1 increases with decreasing misfit and rotate as the orientation changes.

Molecular-dynamics calculations show that at low temperatures the monolayer forms a honeycomb network of domain walls, although the form is less regular than that shown in Fig. 1.[18] The domain walls are not pinned to the substrate and move easily.[18,25] For systems with fixed coverage, this behavior can be described in terms of domain-wall vibrations about a honeycomb configuration with perfect hexagonal symmetry. The lowest-energy deviation of the domain walls from the perfect honeycomb configuration is a breathing distortion which varies the size of the registered domains without changing the total length of the domain walls in the monolayer.[16] If energy is not required to breathe the domain walls, the potential energy will be the same for all breathed configurations and can be calculated from the configuration of smallest periodicity. If the breathing motion requires energy, the periodic configuration will be the configuration of minimum energy. If the periodic configuration has vibrational modes that are unstable, then another configuration will be lower in energy. The energy of the monolayer at a given misfit and orientation is calculated with the assumption that the configuration is periodic. Because the domain walls are free to translate,[25] there will not be a unique periodic configuration of minimum energy. To restrict the calculation, the energy is determined from the periodic configuration that has inversion symmetry about the centers of the registered regions. (Figure 1 is an example of such a configuration.) The assumption that this type of configuration has minimum energy is tested when the vibrational modes of the system are calculated.

As shown by de Wette *et al.*,[26] the krypton monolayer on a graphite substrate will have a variety of vibrational modes. Some modes can be attributed exclusively to vibrations of the adsorbed atoms, some modes can be attributed to the substrate, and some modes involve a coupling between the motions of the monolayer and substrate. The motion of the adsorbed atoms within the plane of the monolayer is decoupled from the substrate and can be calculated with the assumption that the substrate is rigid. The out-of-plane modes, however, in the long-wavelength limit are heavily coupled to the bulk modes of the substrate and cannot be calculated using the rigid-substrate approximation.

The coupling between the out-of-plane monolayer

modes and substrate has also been observed experimentally,[27] although the coupling is less complex than the work of de Wette *et al.*[26] would suggest. For the most part, the out-of-plane motion of the monolayer appears to be *Einstein-like*[28,29] with the only coupling occurring at wave vectors where the Rayleigh mode of the substrate can become hybridized with the motion of the monolayer. This behavior was predicted by Hall *et al.*,[30] who performed calculations for a monolayer on an elastic substrate. They also found that the long-wavelength modes of the monolayer can become broadened in frequency due to a *radiative damping* with the substrate bulk modes. The average value of the out-of-plane mode frequencies do not, however, vary from that calculated by treating the monolayer as an Einstein oscillator on a rigid substrate, except at wavelengths where the substrate Rayleigh mode couples to the motion of the monolayer.

In any case, the experimental evidence indicates that the motion specific to the monolayer appears to be less sensitive to the substrate's dynamics than de Wette *et al.*[26] suggest. (The discrepancy in de Wette's calculation may be due to the fact that only 13 sheets of graphite were used to model the substrate, and the monolayer may thus have an undue influence on dynamics of the total system.) The short-wavelength motion of the monolayer out of the plane is dispersionless, even if the long-wavelength motion may not be.[28,29] This implies that the adatom interactions are insignificant and can be neglected for these modes. This conclusion will be valid for all incommensurate configurations considered in this work, because the compression of the adatoms is never great enough for their interactions to significantly influence the out-of-plane behavior of the monolayer. From Steele's[14] estimates of the substrate corrugation, the influence of corrugation on the substrate interaction is totally overshadowed by the magnitude of the holding potential $V_a(z)$ of the substrate (2), and for the out-of-plane behavior the substrate interaction can essentially be regarded as uniform. It can therefore be said that for motion perpendicular to the substrate the adatoms move independently of each other without regard to their location on the substrate. This removes any possible distinction between out-of-plane motion of adatoms in the commensurate and incommensurate monolayers, and the mode coupling between the monolayer and the substrate is expected to be, on average, the same regardless of the configuration of the monolayer. The out-of-plane dynamics of the monolayer is thus neglected as it has no influence on the configuration of the monolayer.

The average holding potential of the substrate, $V_a(z)$ in (2), which dominates the out-of-plane motion, does not affect in-plane behavior. The behavior of adatoms within the plane is determined by the substrate corrugation and the interactions between the adatoms. Because the positions of the adatoms change with different configurations of the monolayer, the in-plane free-energy contribution will be configuration dependent and the in-plane dynamics of the monolayer must be determined in order to find the equilibrium configuration.

The in-plane modes are also of considerable interest because they are significantly different for the commensurate and incommensurate monolayers. For the commensurate monolayer, each adatom is at an adsorption site. This locks the monolayer on the substrate and does not allow vibrational energies below a given band-gap value. The incommensurate monolayer, however, has highly mobile domain walls and the IC phase has low-energy modes. Indeed, Villain predicted that a domain-wall breathing mode could become completely soft[31] with consequences for the commensurate-incommensurate phase transition.[32] In the following sections, any further mention of dynamics or motion will refer to that within the plane of the monolayer.

III. CALCULATION

A. Static configuration

From (2) the adatoms are forced to lie on a surface $z(\mathbf{r})$. The positions of the adatoms on this surface are determined by interactions between each other, and with the substrate. The variation in height z of the adatoms is so slight that the adatom-pair interactions can be calculated as if the monolayer was planar.[17] The form of the substrate interaction is given by (3). The lateral positions $\mathbf{r}$ of the adatoms for the minimum-energy configuration must satisfy (5). The heights of the adatoms can be subsequently calculated from (2) once their lateral positions are known. To reduce the calculation, only periodic configurations with registered regions that are separated by domain walls which cause a shift of only one adsorption site are considered. Further simplifications to the calculation are possible, because the displacements of the adatoms $\mathbf{u}(\mathbf{R})$ are smoothly modulated and the distances between adatoms remain close to the averaged spacing $\mathbf{R}$ determined from the misfit. The adatom-pair potentials used in (4) and (5) can be expanded as a Taylor series about the averaged spacings,

$$\Phi(\mathbf{r}-\mathbf{r}')=\{1+(\mathbf{u}-\mathbf{u}')\cdot\nabla+\tfrac{1}{2}[(\mathbf{u}-\mathbf{u}')\cdot\nabla]^2+\tfrac{1}{6}[(\mathbf{u}-\mathbf{u}')\cdot\nabla]^3+\cdots\}\Phi(\mathbf{R}-\mathbf{R}') \ . \tag{8}$$

From (6), $\mathbf{u}$ and $\mathbf{u}'$ are functions of $\mathbf{R}$ and $\mathbf{R}'$, respectively, and the gradient operator works on the argument $\mathbf{R}$ of the function Φ. Because the distances between the adatoms remain near the spacing of the triangular lattice, this series can be truncated after the first few terms. The most frequently used truncation for analytic studies excludes the anharmonic terms. This approximation has been discussed in a previous work[33] with the conclusion that the expansion of (8) must include at least the cubic term to produce agreement with relaxation studies.[17]

Other studies on similar systems have considered the quartic term and have concluded that truncating (8) at the cubic term is adequate.[34] Therefore, to allow the influence of pair interactions to be calculated rapidly, all terms past the cubic one are neglected.

Another benefit of the smooth modulation in the adatom positions is that the amount of information required to describe the configuration of the monolayer can be reduced.[20] From the periodicity of the monolayer, the displacements of adatoms $\mathbf{u}(\mathbf{R})$ can be expressed as a Fourier sum,[20,35]

$$\mathbf{u}(\mathbf{R})=\sum_{l,m}\mathbf{u}_{lm}e^{i\mathbf{q}_{lm}\cdot\mathbf{R}}\ , \tag{9}$$

where $\mathbf{q}_{lm}=l\mathbf{q}_1+m\mathbf{q}_2$ is a reciprocal-lattice vector of the superlattice. The Fourier series can be truncated after the first few long-wavelength shells because the displacements have such a smooth spatial modulation. Inversion symmetry about the centers of the registered regions is assumed so that $\mathbf{u}_{l,m}=-\mathbf{u}_{-l,-m}$. The resulting reduction in the amount of information required to describe the system makes the computations for the displacements $\mathbf{u}$ more efficient. The values of $\mathbf{u}_{lm}$ are then determined through a Newton step process which finds the values for which the total force on each adatom is zero.[33,35] The consequences of assuming that the minimum-energy configuration is periodic with inversion symmetry about the registered centers is discussed later when the vibrational modes of the system are considered.

B. Dynamic contributions

The static positions so determined provide a basis about which the dynamic nature of the monolayer can be examined. Krypton atoms are quite massive and at low temperatures their vibrational amplitudes relative to their neighbors will be small. Calculations of the dynamics of floating monolayers indicate that anharmonic effects provide only a small perturbation to the general results obtained from harmonic treatments.[36] Thus, at low temperatures, the general behavior of the adatoms in response to each other can be obtained if the force constants are assumed to be harmonic.

For incommensurate monolayers, the adatoms are also influenced by the substrate. The domain-wall motion causes significant movement of the adatoms relative to the surface and the influence of the substrate interaction will be harmonic only for small displacements of the walls. Since the walls move freely,[25] the energy associated with their motion will be small and the amplitude of their vibrations will be large, even at zero temperature. As a result, the influence of the substrate interaction on the motion of the adatoms will not be harmonic. This, however, does not imply that the mode frequencies cannot be calculated with the harmonic approximation.

From a renormalized description of the incommensurate monolayer, the properties of the monolayer can be determined entirely from the shape of its domain-wall structures. The location of these structures on the substrate is not relevant because the pinning is so small.[25] In the renormalized picture, the domain walls will have vibrational modes associated with their motion. Since the behavior of the domain walls is insensitive to their location on the substrate, anharmonic effects will result only from the walls colliding. The following calculation assumes that these collisions do not occur and the motion of the domain walls is harmonic. The vibrational frequencies can then be determined by considering infinitesimal perturbations of the domain-wall system. Under such conditions the interactions on the adatoms vary harmonically, and the forces on the adatoms can be determined from a dynamical matrix based on their static force-free positions.

The vibrational modes of the monolayer are calculated from the dynamical matrix. The positions of the vibrating adatoms are defined to be

$$\mathbf{r}(\mathbf{R},t)=\mathbf{r}(\mathbf{R})+\mathbf{v}(\mathbf{R},t)\ , \tag{10}$$

where $\mathbf{r}(\mathbf{R})$ is the static force free position of (6) and $\mathbf{v}(\mathbf{R},t)$ provides the time-dependent behavior. With the assumption of harmonic behavior, the motion of the adatoms satisfy

$$M\frac{\partial^2}{\partial t^2}\mathbf{v}(\mathbf{R},t)=-\sum_{\mathbf{R}'}\underline{D}(\mathbf{r}(\mathbf{R}),\mathbf{r}(\mathbf{R}'))\cdot\mathbf{v}(\mathbf{R}',t)\ , \tag{11}$$

where M is the mass of the adatom, $\underline{D}$ is the dynamical matrix of the superlattice, and the summation over $\mathbf{R}'$ includes the point $\mathbf{R}$.

The method of solving (11) for the lowest-energy vibrational modes has been described in a previous paper.[25] The solutions provide the in-plane normal modes $(\omega_s(\mathbf{k}),\mathbf{v}_{lm}(s,\mathbf{k}))$ of the system. The index s is used to identify the mode: Because the system is two dimensional, the number of modes will be twice the number of adatoms per domain. Although $\omega_s(\mathbf{k})$ is the frequency of the mode, the low-frequency motion of the domain walls will not be given directly by $\mathbf{v}_{lm}(s,\mathbf{k})$. Instead, the form of the domain-wall motion must be interpreted from the harmonic movement of the adatoms on the domain walls.

With the low-energy vibrational frequencies, the in-plane component of the average Helmholtz free energy per adatom can be calculated from

$$f_c=U_c+\frac{\hbar}{2N}\sum_{s,\mathbf{k}}\omega_s(\mathbf{k})+\frac{1}{N\beta}\sum_{s,\mathbf{k}}\ln(1-e^{-\beta\hbar\omega_s(\mathbf{k})})\ , \tag{12}$$

where $F_c=Nf_c$ for Eq. (1), and U_c is the energy per adatom of the static configuration. Equation (12) has split the free energy into a static energy contribution U_c, a zero-point energy E_0, and a temperature-dependent contribution E_T. The static energy, U_c, has been discussed in the preceding subsection. The calculation for the temperature-dependent contribution, E_T, involves only the lowest-energy vibrational modes. These mode energies are calculated and the value of E_T is obtained by summing over the $\mathbf{k}$ vectors in the superlattice Brillouin zone. This summation is made more efficient by extracting the logarithmic singularity in $\mathbf{k}$ of E_T, which can be directly integrated. The remaining expression is analytic and can be efficiently evaluated numerically by restricting the summation to special $\mathbf{k}$ points in the Brillouin zone.[37,38]

From (12) the zero-point-energy contribution, E_0, involves a summation of all the eigenvalues of the dynamical matrix averaged over all values of wave vector $\mathbf{k}$ in the Brillouin zone. For incommensurate monolayers, the number of adatoms per domain increases dramatically as the density of the configuration approaches the commensurate limit. As an example, the nonrotated configuration with a misfit of 2.22% has 675 adatoms per domain and thus 1350 in-plane normal modes. Solving for all the eigenvalues of such a large system is computationally unwieldy. Furthermore, calculating the eigenvalues for several $\mathbf{k}$ points compounds the problem. Therefore, a more practical method of calculating E_0 is required.

If the eigenvalues of the dynamical matrix are defined to be $\lambda_s(\mathbf{k})$, the frequency $\omega_s(\mathbf{k})$ of the mode can be determined from

$$\lambda_s(\mathbf{k})=M\omega_s^2(\mathbf{k}) , \tag{13}$$

where M is the mass of an adatom. The zero-point energy can then be expressed as

$$E_0=\frac{\hbar}{2\sqrt{M}}\int_{\lambda_0}^{\lambda_m} g(\lambda)\sqrt{\lambda}\,d\lambda , \tag{14}$$

where λ_m and λ_0 are the upper and lower bounds of $\lambda_s(\mathbf{k})$, respectively, and $g(\lambda)$ is the density of states.

The density of states, being a function of λ, can be expanded as a sum of orthogonal polynomials. In the case of two-dimensional systems, $g(\lambda)$ is nonzero at its minimum, λ_0, and maximum, λ_m. Functions of this form are well described using Legendre polynomials,[39]

$$g(\lambda)=\sum_{n=0}^{\infty} a_n P_n(2(\lambda-\lambda_a)/\lambda_d) , \tag{15}$$

where $\lambda_a=(\lambda_m+\lambda_0)/2$, $\lambda_d=\lambda_m-\lambda_0$, and a_n must have the form

$$a_n=\frac{2n+1}{\lambda_d N}\sum_{s,\mathbf{k}} P_n(2(\lambda_s(\mathbf{k})-\lambda_a)/\lambda_d) . \tag{16}$$

The factor of $1/N$ indicates that the summation is actually an average over all modes s and wave vectors $\mathbf{k}$ in the superlattice Brillouin zone. Using the form (15) for $g(\lambda)$ in (14) produces

$$E_0=\frac{\hbar}{2\sqrt{M}}\sum_{n=0}^{\infty} a_n c_n(\lambda_m,\lambda_0) , \tag{17}$$

where

$$c_n(\lambda_m,\lambda_0)=\int_{\lambda_0}^{\lambda_m}\sqrt{\lambda}P_n(2(\lambda-\lambda_a)/\lambda_d)d\lambda . \tag{18}$$

Thus, E_0 can be calculated once the orthogonal polynomial moments a_n of the dynamical matrix are determined. While many moments may be required to accurately describe the density of states $g(\lambda)$ in (15), calculations of smooth averages require relatively few moments and (17) provides an efficient means of obtaining E_0.[39] The moments a_n can be obtained by the method of Wheeler and Blumstein,[40] which expresses the summation over s in (16) as the trace of an orthogonal polynomial matrix. More details about the calculations in this work are given in Ref. 41.

IV. BEHAVIOR OF THE MONOLAYER

A. Zero-temperature properties

The krypton atoms upon adsorption by the monolayer will settle into a configuration for which the free energy is minimized. At finite temperatures the density of the monolayer varies as a function of the krypton-vapor chemical potential. For systems at equilibrium, this relationship is governed by the monolayer's energy variation with misfit. At zero temperature essentially all krypton atoms will be adsorbed onto the substrate. For a totally covered substrate the monolayer's density will therefore be dependent only on the number of krypton atoms in the system. As more krypton atoms are added, the density increases. At submonolayer densities the krypton atoms form solid islands which possibly are surrounded by a lattice gas of krypton atoms. If the average energy per adatom of a solid incommensurate configuration is lower than the energy of the commensurate configuration, the islands will be incommensurate; otherwise, the islands will be commensurate.

Plots of the energy per adatom as a function of misfit for a variety of substrate corrugations are shown in Figs. 2(a)–(2d). The dashed curves show the potential energy per adatom, while the solid lines include the zero-point energy. If the influence of the zero-point energy is disregarded, the substrate corrugation must be at least 9.8 K for the monolayer to have a commensurate configuration. (This value is different from the value of 11.0 K reported by Gooding *et al.*[17] because a more accurate form is used for the substrate screening of the adatom interaction.) When the influence of the zero-point energy is included, however, the critical substrate corrugation required to permit a commensurate configuration is reduced to 7.0 K. This indicates that the substrate-corrugation value of 7.4 K calculated by Vidali and Cole[42] is sufficient to ensure that the monolayer has a commensurate phase at low temperatures.

The dependence of the zero-point energy on misfit is shown in Figs. 3(a) and 3(b). That the zero-point energy should increase with misfit is not unexpected because the force constants between the adatoms increase as the density is increased. The zero-point energy does not change as the monolayer is rotated, and because of this it was expected that a calculation based on a floating monolayer with an averaged substrate influence would duplicate the results of Fig. 3. Such a calculation was performed, and although it reproduced the general trend in the zero-point energy, a more rigorous treatment is required if the actual values are to be matched. The behavior of the zero-point energy matches that of a floating monolayer if the misfit is large enough that distinct domain walls are not formed [Fig. 3(a)]. For smaller misfit values the zero-point energy appears to vary linearly with misfit as it approaches the commensurate transition. Because of computational constraints, zero-point energies cannot be determined close to the transition and the curves have been extended to meet the commensurate values [Fig. 3(b)]. The zero-point energy may thus not vary linearly close to the transition. However, if the zero-point energy

per domain can be expressed as a summation of the zero-point energy of the registered region and the zero-point energy of the adatoms on the domain walls, from a renormalized domain-wall argument, the zero-point energy should vary linearly with misfit close to the commensurate transition.

The orientational epitaxy has been analyzed for three different substrate corrugations which represent the general behavior of the monolayer. Selective data have been calculated for other V_g values to confirm the trends illustrated. The energy of the monolayer is relatively insensitive to its orientation. In order to separate the orientational behavior from the misfit-dependent behavior, the results are displayed as energy differences between the rotated configuration and the nonrotated configuration. The energy differences are mapped out as contours on a surface of possible misfits and orientations [Figs. 4(a)–4(c)]. The path of minimum energy is indicated by the thick dashed line. The thin dashed line indicates the path of minimum enenergy if the adatom pair interactions are assumed to be harmonic (these are the curves that Shiba's theory would predict). The energies corre-

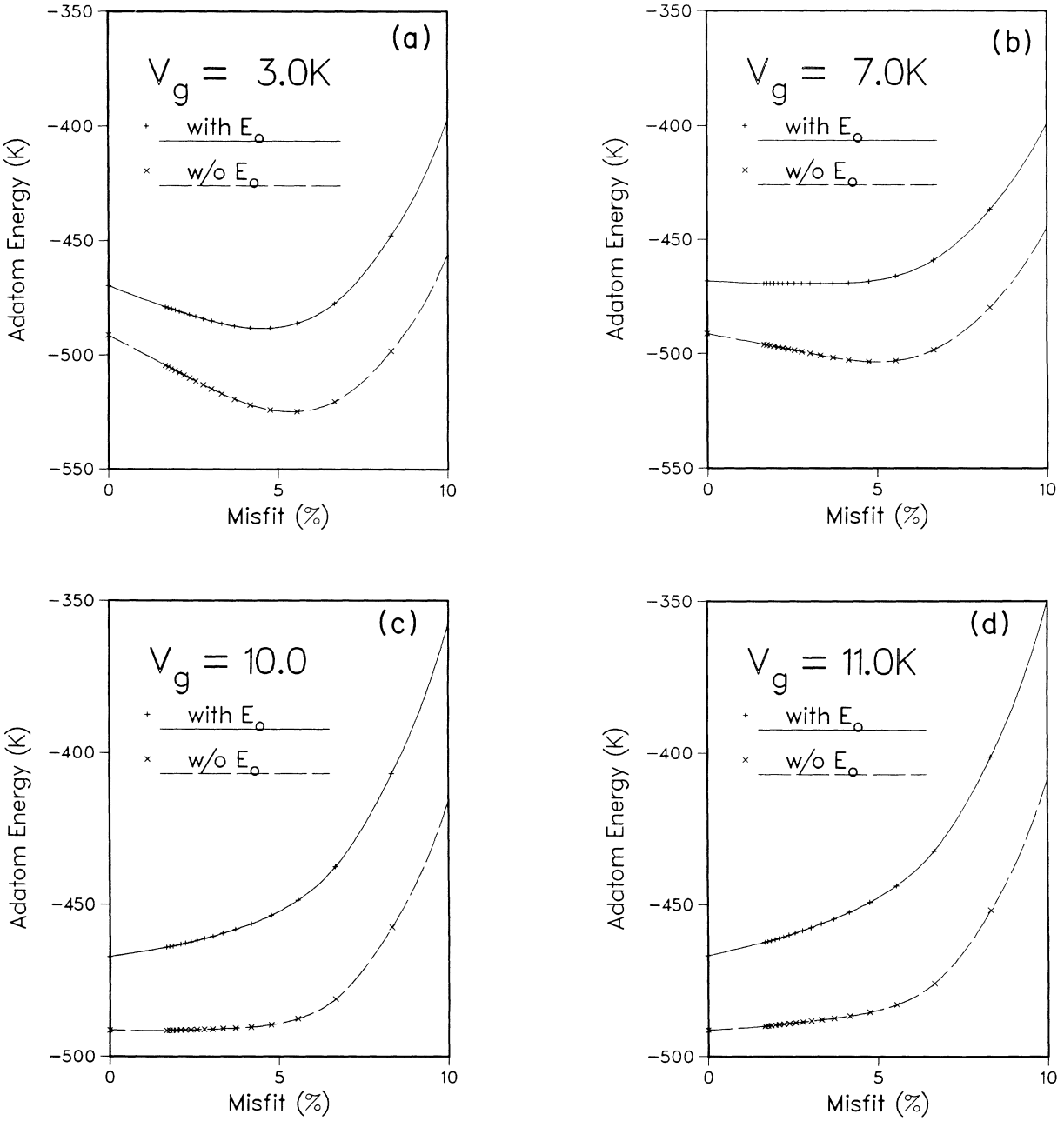

FIG. 2. (a) Energy per adatom of a nonrotated incommensurate monolayer as a function of its misfit ε when the substrate corrugation V_g is 3.0 K. The dashed line shows the potential energy per adatom, the solid line shows the potential energy plus zero-point energy per adatom. (b) As in (a), but with $V_g = 7.0$ K. (c) As in (a), but with $V_g = 10.0$ K. (d) As in (a), but with $V_g = 11.0$ K.

sponding to a harmonic calculation are shown in Fig. 4(d); the substrate corrugation used in the calculation is 10.0 K, although the results of the harmonic calculation are general to other substrate corrugations if the axes are scaled accordingly. The ragged appearance of the zero contour at low angles and misfits is a consequence of the fact that the energy variation becomes so slight that the calculational inaccuracies become apparent.

The energy of the monolayer increases sharply as the monolayer's orientation is increased past that of the minimizing angle. The calculational procedure breaks down, however, as orientations which correspond to heavy-wall configurations are reached. This breakdown occurs because the calculation assumes that the adatoms are only slightly displaced from a triangular lattice configuration [Eq. (6)]. Because the adatoms resist shearing much less than they resist compression, for such highly rotated configurations the shear can become quite sharp. These violent shifts cannot be described by our procedure, which assumes that the displacements of the adatoms are small and smoothly varying. Fortunately, this problem is not of consequence because heavy-wall configurations are significantly higher in energy than the nonrotated configurations.[17] Thus, the orientations that can be considered within the constraints of the calculation are sufficient to determine the equilibrium configurations of the monolayer.

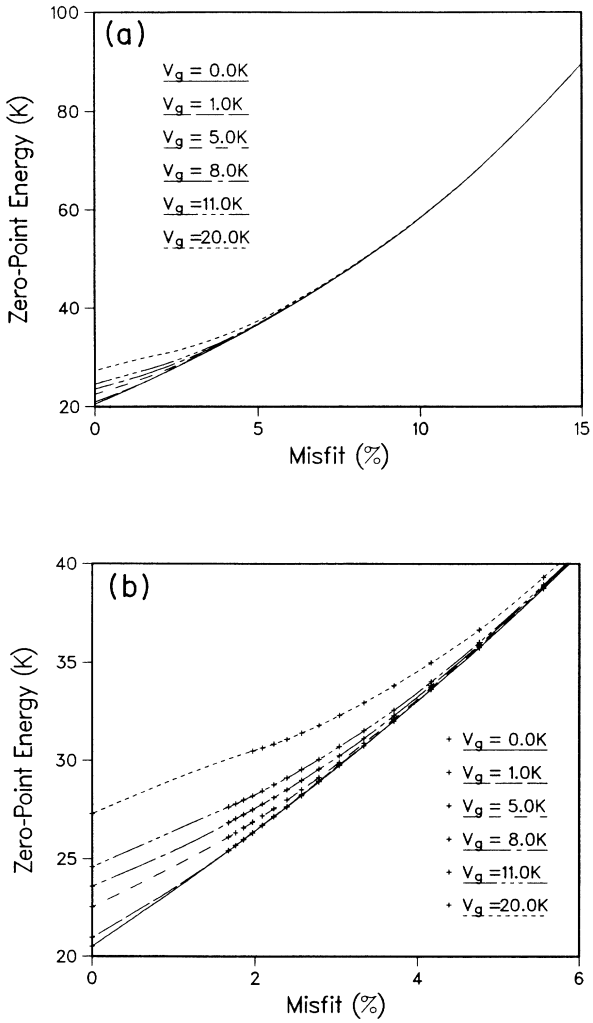

FIG. 3. (a) Zero-point energy per adatom as a function of misfit ε for a variety of substrate corrugations V_g. (b) As in (a), but showing more details of the low-misfit region.

For substrate corrugations approaching zero, the orientational behavior of the monolayer matches that predicted by Novaco and McTague.[43] As the substrate corrugation is increased, however, the more general theory of Shiba[20] must be used to describe the behavior. When the substrate corrugation has a value $V_g = 5.0$ K, the minimum-energy path matches closely the behavior predicted by Shiba.[20] This is expected because harmonic theories are found to be adequate for such a corrugation.[33] However, for larger corrugations the behavior changes and the monolayer rotates at misfits much smaller than Shiba's theory would predict. Furthermore, the line shape of the minimum-energy configuration's rotation-versus-misfit curve will not match the Shiba result even if an arbitrary scaling of Shiba's parameters is used. To understand this behavior the structure of the monolayer must be considered.

A general analysis of the structure of nonrotated monolayers of small misfit reveals that the density of the adatoms is constant at the center of the domains, it increases along the domain walls, and reaches a maximum at the vertices. This is in agreement with the concept of soliton density modulations arranged in a honeycomb network.[44] The peak in density at the vertex is due to the focused compression of the domain walls which intersect at the vertex. The compression of the adatoms at the vertices becomes stronger for higher substrate corrugations and the spacing of the adatoms at the vertex becomes less than 4.03 Å (the spacing favored by the floating monolayer). For example, when $V_g = 8.0$ K the spacing at the vertex is found to be 3.99 Å and the adatoms are overcompressed. If the monolayer is allowed to rotate, the domain walls form a staggered intersection[45] and the compression due to the domain walls is diffused. The density of the adatoms at the vertices for rotated configurations is not as high as that for the nonrotated configuration and spacings closer to 4.03 Å are found. This decreases the interaction energies of the adatoms at the vertices, and because the change in the substrate-energy component due to diffusing the vertex is negligible, the rotated configuration has lower-energy vertices. Gordon and Lançon[45] have considered the diffusion of the vertex in relaxation calculations. They conclude that rotating the monolayer slightly does not cause any observable change in energy. However, as seen in Figs. 4(a)–4(c) the energy difference is very slight and, within the accuracy of their calculation, they may not have detected this effect.

If the vertices do become overcompressed, when the misfit is large the monolayer has relatively many vertices and the rotated configurations will be energetically more favorable. For smaller misfits the preferred configuration becomes nonrotated despite the overcompression of the

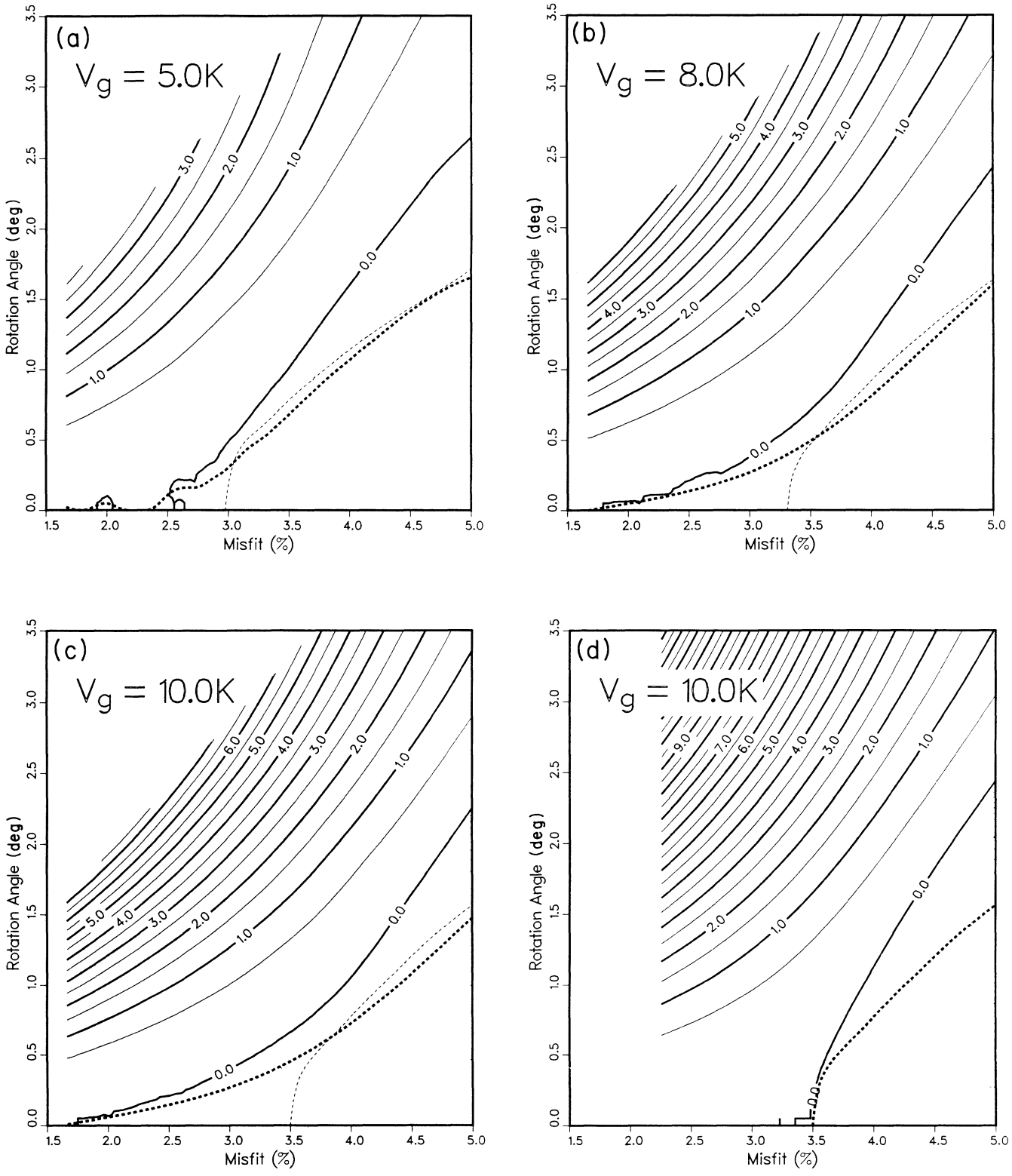

FIG. 4. (a) Contour plot showing the difference in the energy (potential plus zero point) per adatom between the rotated and nonrotated configurations. The solid contours show increments of 0.5 K. The dotted contours show decrements of 0.02 K. The substrate corrugation V_g for this plot is 5.0 K. The path of minimum energy is shown by the thick dashed line, the minimum energy path corresponding to Shiba's theory is shown as a thin dashed line. (b) As in (a), but with $V_g = 8.0$ K. (c) As in (a), but with $V_g = 10.0$ K. (d) As in (a), but with $V_g = 10.0$ K. Also, in this last figure, the adatom-pair potential used in the calculation is a harmonic approximation to the actual potential. The thick dashed line shows the path of minimum energy and is equivalent to that predicted by Shiba's theory.

vertices. This is due to the fact that the number of adatoms at the vertices becomes significantly less than the number of adatoms on the domain walls. Because the domain walls for rotated configurations must contain a shear as well as a compression, the domain-wall adatoms would favor a nonrotated configuration. At smaller misfits, the adatoms on the domain walls dominate the adatoms at the vertices and the monolayer becomes nonrotated. This describes the orientational behavior found in Figs. 4(b) and 4(c).

As noted previously, this orientational behavior is not in agreement with the predictions of Shiba.[20] This discrepancy is directly attributable to the anharmonic nature of the pair potential. In harmonic theories the sharp potential minimum of the adatom interaction is not well modeled. However, including the cubic term improves the fit considerably.[41] Additional terms in the Taylor-series expansion will add to the accuracy, but as noted previously, their contribution will be slight compared to the impact of including the cubic term. Thus, for a periodic system, additional improvements in the theory due to including more Taylor-series terms will only cause slight changes in the misfit value for the onset of rotation. The question remains, however, whether the monolayer can be considered periodic with inversion symmetry about the domain centers. The vertices can also be diffused if the domain walls are translated with respect to the substrate. This breaks the inversion symmetry of the monolayer. This possibility is discussed in the next section.

Experimentally, the orientational behavior is observed to match the results of Shiba.[9,12] Because the measurements were taken at fairly high temperatures (>30 K), the thermal motion of the adatoms should diffuse the vertices and allow the nonrotated phases to be favored, whereas the zero-temperature results shown in Figs. 4(b) and 4(c) would indicate otherwise. This is not unreasonable because the domain walls are predicted to broaden with temperature.[21,46] The orientational behavior should thus be susceptible to the temperature of the monolayer. The misfit value at which the monolayer starts to rotate will increase as the temperature of the monolayer is increased. This type of behavior is observed, with the experimental results of Fain *et al.*[9] taken at 52 K showing an onset of rotation much less than the 89-K results of d'Amico *et al.*[12] The results of Schabes-Retchkiman and Venables[10] do not follow this trend, but their use of graphite flakes instead of a single crystal may have resulted in edge effects dominating the orientational behavior. For this behavior to be properly verified, the misfit value of the onset of rotation should be measured at a variety of temperatures on the same single-crystal substrate.

B. Vibrational instabilities

The vibrational modes of the monolayer are important not only because they reveal the dynamical behavior of the system, but also because they indicate if the static configuration about which they are determined is stable. It is remembered that the monolayer configurations were calculated with the assumption that the lowest-energy

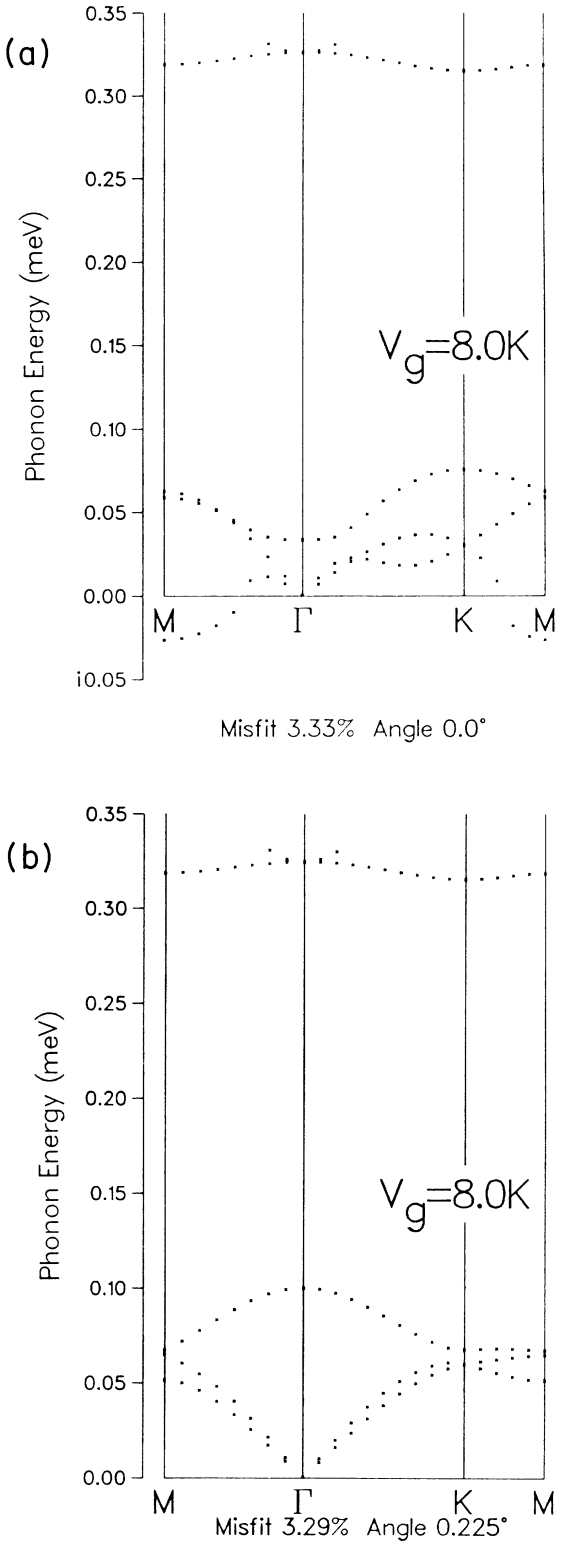

FIG. 5. (a) Vibrational energies as a function of wave vector for a nonrotated incommensurate monolayer with misfit 3.33% and substrate corrugation 8.0 K. Γ is at the center of the hexagonal Brillouin zone, M is at the middle of and edge, and K is at a corner. The energy scale is extended to show imaginary values. (b) As in (a), but the monolayer is rotated 0.225° with respect to the substrate and the misfit is 3.29% [slightly less than in (a)].

configuration had inversion symmetry about the centers of the registered domains. For substrate corrugations less than 7.0 K, all configurations examined were stable regardless of the misfit or orientation. Thus, imposing inversion symmetry on the monolayer's configuration will not compromise the calculated equilibrium value of the energy per adatom at any misfit or orientation when the substrate corrugation is less than 7.0 K.

When the substrate corrugation is greater than 7.0 K, one of the vibrational modes becomes unstable for nonrotated or slightly rotated configurations when the misfit of the monolayer is less than 3.5%. Dispersion curves of a representative configuration are shown in Fig. 5(a), with the form of the unstable mode shown in Fig. 6. The nonrotated configurations do become stable when the misfit is reduced past 2.5%, although this fact was confirmed only for substrate corrugations between 8.0 and 11.0 K. Also, as shown in Fig. 5(b), when the monolayer is rotated sufficiently, the shearing mode of Fig. 6 becomes stable.

From the preceding discussion of the orientational behavior of the monolayer, the nonrotated configurations of the monolayers are not favored because the vertices are overcompressed. It is possible to diffuse the vertices without rotating the monolayer by translating the domain walls relative to the substrate. This would break the inversion symmetry. If the energy of the monolayer could be reduced by shifting the domain walls, the translational modes of the monolayer would be unstable. These modes, from Fig. 5(a), are not unstable; instead, it is a shearing mode (Fig. 6) that is unstable. This indicates that the domain walls do not resist shearing, and are prone to rotate. This is expected because the energies of the rotated configurations are lower in energy whenever the monolayer is found to be unstable.

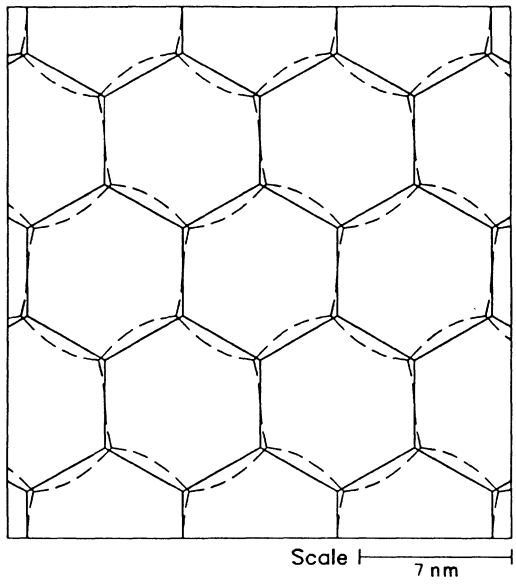

FIG. 6. Motion of the domain walls for the unstable mode at the M point in Fig. 5(a). The dashed lines indicate the deformation of the domain walls about their central positions (solid lines). In this picture, the direction of the wave vector is along the vertical line from the zone center. (The scale is provided to indicate the size of the domains; the magnitude of the deformation has been scaled arbitrarily to make its form visible.)

The overcompression of the vertices is therefore a significant influence, not only on the static energy of the monolayer, but also on the stability of the configuration. The monolayer will seek to ease the overcompression by rotating rather than breaking the symmetry imposed on the configuration. At higher temperatures, thermal motion of the adatoms is expected to diffuse the vertices so that the periodic nonrotated configurations become stable. Such an effect requires a self-consistent phonon calculation, and confirmation of this prediction awaits further work.

C. Finite-temperature properties

The temperature dependence of the energy per adatom is provided by the last term (denoted E_T) in Eq. (12), with the other terms providing the zero-temperature energy per adatom. From (1), once the variation in the free energy per adatom with misfit is known, the equilibrium misfit of the monolayer can be determined from the chemical potential. Experimentally, the misfit ε is found to vary with the chemical potential μ as

$$\varepsilon = A(\mu - \mu_c)^{\beta}, \tag{19}$$

μ_c being the chemical potential of the commensurate configuration. A and β are parameters that are insensitive to the pressure or temperature of the system.[4,9,11] For the free energy of (1) to have a minimum at misfit values which vary with chemical potential as (19), the free energy per adatom, $f_c(\varepsilon)$, from (12) must have the form

$$f_c(\varepsilon) = \mu_c + (1-\varepsilon)^2 \left[a + c \int^{\varepsilon} \frac{x^{\sigma}}{(1-x)^3} dx \right], \tag{20}$$

where $\beta = 1/\sigma$ and $A = (2/c)^{\beta}$.

For reasonable values of the substrate corrugation, over the range of misfit values examined experimentally, the monolayer goes from a modulated structure to a domain-wall network as the misfit is decreased. It has been suggested by Villain[31] that the observed variation of the monolayer's misfit with chemical potential is merely a result of the monolayer undergoing the transition from being a modulated structure to being a domain-wall network. This explanation has not be accepted as being complete, because the energetics of the domain-wall network is expected to be significant at lower misfit values, and because for misfit values near the crossover the behavior of the monolayer is expected to vary with temperature.

The energies of the low-energy modes have been calculated in this work for a variety of monolayer configurations: From Eq. (12) their contribution to the free energy is provided by the term E_T. At low temperatures, the magnitude of E_T is extremely sensitive to errors in the calculated frequencies of the low-energy modes. Because of the approximations to the normal-mode calculation required to keep the computation

TABLE I. Values of E_T calculated for various temperatures and orientations when $\varepsilon = 3.7\%$.

	$T=0.5$ K	$T=1.0$ K	$T=2.0$ K	$T=4.0$ K
$\theta=0.00°$	−0.0019 K	−0.0086 K	−0.0325 K	−0.1329 K
$\theta=0.52°$	−0.0011 K	−0.0058 K	−0.0252 K	−0.1171 K
$\theta=0.79°$	−0.0011 K	−0.0055 K	−0.0240 K	−0.1145 K
$\theta=0.95°$	−0.0009 K	−0.0051 K	−0.0231 K	−0.1130 K

manageable, when the misfit is small or the substrate corrugation is large the low-frequency values obtained will not be accurate.[25] Thus the calculations are constrained to configurations with larger misfit values and/or smaller substrate corrugations.

The calculation of E_T is also not possible if the underlying static configuration is unstable. When the substrate corrugation is greater than 7.0 K, the nonrotated configurations become unstable when the misfit is between 2.5% and 3.5%. Thus the calculation for E_T is confined to stable configurations that permit the frequencies to be determined accurately.

The configurations chosen for this study have misfits of 2.8%, 3.0%, and 3.7%. When the misfit is 2.8% or 3.0%, only rotated configurations are considered. The substrate corrugation is taken to be 8.0 K, so that the domain walls are clearly separated at 2.8% misfit, while the configuration at 3.7% is a modulated structure. This allows the free energy associated with soft-domain-wall modes to be compared to the more rigid system that does not have distinct domain walls.

The values E_T for these configurations are shown in Tables I–III. The immediate observation can be made that at low temperatures the contribution of E_T to the free energy will be negligible. The only impact that the domain-wall modes can have is perhaps to change the equilibrium orientation of the monolayer. More significantly, the rapid softening of the domain-wall modes does not cause any appreciable increase in the values of E_T.

The values of E_T have not been determined for temperatures greater than 4.0 K. This limit has been imposed since no modes are calculated with energies greater than twice the commensurate band-gap value of 11.0 K. This commensurate band-gap value is the lowest possible energy that the modes of the commensurate monolayer can have when the substrate corrugation is 8.0 K. Because the accuracy of the frequencies deteriorates with increasing energy, values with energies much greater than the band gap will be suspect. Furthermore, additional modes may be present in the monolayer that are missed by the calculation. Thus the temperatures must be kept small so the inaccuracies caused by the approximations required to solve Eqs. (11) are minimized.[25]

The frequencies have been calculated under the assumption of harmonic motion. This approximation will not be valid if the domain walls collide with each other. Since collisions of the domain walls will increase the energy of wall modes, anharmonic effects are expected to diminish the values of E_T. Confirmation of this prediction awaits a self-consistent phonon calculation of the incommensurate monolayer.

The only mechanism that could soften the domain-wall motion is the formation of domain-wall dislocations.[32] Further work based on the elastic constants of the renormalized domain-wall system should be performed. In the absence of domain-wall dislocations, however, at low temperatures domain-wall motion will not influence the misfit and orientation for the equilibrium configuration of the monolayer.

To extend the results closer to the commensurate limit, it is necessary to estimate the change in E_T as the misfit decreases. From previous work,[25] when the domain size is large the softest mode is the breathing mode. At low temperatures this mode will dominate the value of E_T and the variation of its contribution due to misfit must be examined. The breathing mode is influenced by the domain-wall interaction. The strength of this interaction will decrease as

$$U_w(L)=cL^{\sigma}e^{-\kappa L} \tag{21}$$

for increasing separation L of the domain walls.[21] The constants c, σ, and κ are determined from the calculated energetics of the system. Correspondingly, the frequency of the breathing motion should decrease as

$$\omega(\mathbf{k})=f(\mathbf{k},L)e^{-\kappa L/2}\ , \tag{22}$$

where $f(\mathbf{k},L)$ is a function which is periodic in $\mathbf{k}$ and algebraic in L. To leading order, the contribution of this mode to E_T will decrease as

$$\frac{1}{N_p}\ln(e^{-\kappa L/2}) \tag{23}$$

with increasing L. Since N_p (the total number of modes) varies as L^2, the contribution will decrease as $1/L$. This analysis assumes that the harmonic approximation for

TABLE II. Values of E_T calculated for various temperatures and orientations when $\varepsilon = 3.0\%$.

	$T=0.5$ K	$T=1.0$ K	$T=2.0$ K	$T=4.0$ K
$\theta=0.09°$	−0.0034 K	−0.0116 K	−0.0366 K	−0.1419 K
$\theta=0.71°$	−0.0020 K	−0.0073 K	−0.0260 K	−0.1192 K

TABLE III. Values of E_T calculated for various temperatures and orientations when $\varepsilon=2.8\%$.

	$T=0.5$ K	$T=1.0$ K	$T=2.0$ K	$T=4.0$ K
$\theta=0.21°$	−0.0022 K	−0.0081 K	−0.0276 K	−0.0941 K
$\theta=0.68°$	−0.0024 K	−0.0080 K	−0.0265 K	−0.0916 K

motion is valid: For low-energy modes the vibrational amplitudes will be large even at zero temperature, and the domain walls may collide with each other. If collisions occur, the motion will not be harmonic and (23) will not be correct.

Coppersmith *et al.*[32] have presented a model which describes the domain walls as being free to move provided that their displacements do not exceed $L/4$. This ensures that the domain walls move independently of each other, and to some extent, simulates an anharmonic repulsion between domain walls. They predict that the free-energy contribution of the domain-wall breathing will decrease as $\ln(L)/L^2$. This is a more restricting limit than $1/L$ predicted by (23) and should be valid for configurations approaching the commensurate transition. The value of E_T at low temperatures is therefore expected to decrease with misfit from the presented values even in the commensurate limit.

At higher temperatures, other domain-wall modes begin to influence the value of E_T. More low-energy domain-wall modes appear as the domain size increases,[25] and the value of E_T could be expected to increase as well. However, the number of these modes does not increase as quickly as the total number of modes, N_p, and, from its form in (12), E_T is still expected to remain small as the domain size increases.

The results presented are for configurations where the substrate corrugation is 8.0 K. Because the domain-wall modes decrease in energy as the value of V_g increases, E_T will increase with V_g. For reasonable values of V_g, the change in E_T can be estimated from a soliton continuum description of the domain wall.[44] Increasing the substrate corrugation will sharpen the domain walls: Given the continuum model, the configuration will resemble a configuration that has a lower value of V_g and smaller misfit. Because κ in (21) varies as $(V_g)^{1/2}$, scaling considerations based on the number of adatoms per domain predict the ratio of N_p for these two configurations to be

$$\frac{N_p}{N_p'}=\frac{V_g'}{V_g} . \tag{24}$$

The vibrational frequencies of the domain walls are expected to be different for the two configurations because the number of adatoms on the domain walls change. The effect of this on E_T, however, is expected to be minor compared to the impact of rescaling N_p. Because the substrate corrugation cannot be significantly greater than 8.0 K, the values of E_T for these configurations should remain small. Correspondingly, it is obvious that decreasing the substrate corrugation will decrease the value of E_T.

Plots of the free energy per adatom as a function of misfit for a variety of substrate corrugations are shown in Fig. 7(a). Because the influence of temperature is so slight, the effect of temperature cannot be shown and the points plotted are the zero-temperature energies. The curves represent the best fit of the parametrized energy form (20). The values of A and β corresponding to the curves are indicated in the legend. It is clear that the energy variation of the floating monolayer ($V_g=0.0$ K) will not produce the experimentally observed misfit–chemical-potential relationship. Furthermore, a high substrate corrugation ($V_g=20.0$ K) does not match the experimental findings either. For intermediate substrate corrugations, however, the values of A and β closely match the experimental values of $A=0.79\%$ and $\beta=0.33$.[4,9,11]

The values of A and β which provide the best fit to the data are extremely sensitive to the range of misfit values considered. If the range is extended to higher misfit values, as shown in Fig. 7(b), the curves for large substrate corrugations also begin to match the experimental results, although the parametrized form of (20) is less adequate to describe such a large misfit variation. If on the other hand, the behavior of the $V_g=20.0$ K data is examined in greater detail at small misfits, the value of β in (20) approaches 1. For such misfit values, the domain walls are sharply defined, and their interactions with each other are reduced: The energy of the monolayer as calculated should depend only on the length of the domain walls and the number of vertices. This type of energy variation will correspond to β having a value of 1 to leading order in (20).[47] It is clear, therefore, that the monolayer must have strongly interacting domain walls which at larger misfit values blend to form a modulated structure if the energy-versus-misfit variation is to produce the experimentally observed behavior. On the other hand, if the substrate corrugation is such that the monolayer undergoes a transition from interacting domain walls to a modulated structure within the range of misfit values considered, the energy-versus-misfit behavior matches that predicted by the experimental finding. This holds true for a broad range of substrate corrugations (1.0–20.0 K and perhaps higher).

To display the influence of the zero-point energy on the misfit variation with chemical potential, plots which consider only the static potential energy per adatom are shown in Fig. 7(c). It is apparent that the values of A and β which provide the best fit to the data do not agree well with the experimental results. The zero-point energy cannot therefore be neglected in calculations for the low-temperature free energy of the system. This fact must be taken into account when qualitatively assessing the results of molecular-dynamics calculations.

It is be to remembered, however, that the experimental

data are obtained at temperatures significantly higher than those considered in this work. At higher temperatures, the higher-energy motion of the adatoms becomes significant. In particular, the adatoms in the registered regions of the monolayer can have significant motion. This type of motion is shown by Schöbinger and Koch[46] to effectively reduce the value of V_g as the temperature is increased. They find that for parameter values which match the wall widths determined by Abraham,[48] the strength of the substrate corrugation at 100 K is reduced to 40% of the value at 0 K. Additionally, as the temperature is increased, the thermal expansion of the adatoms becomes significant and the monolayer can become commensurate when zero-temperature calculations would predict otherwise. Thus the behavior of the monolayer could be expected to vary significantly with temperature.

The experimental work, on the other hand, reveals that temperature only influences the value of the chemical potential μ_c at which the monolayer becomes incommensurate. Temperature does not influence the value of β, at least over the temperature range (52–100 K) of the experimental work. The experimentally observed temperature variation of the value of μ_c can be ascribed to the thermal expansion of the monolayer. From continuum models, the variation in the domain-wall widths can be described in terms of a rescaling of the substrate corrugation. Given the results of this work, as long as the monolayer crosses over from a domain-wall network to a modulated

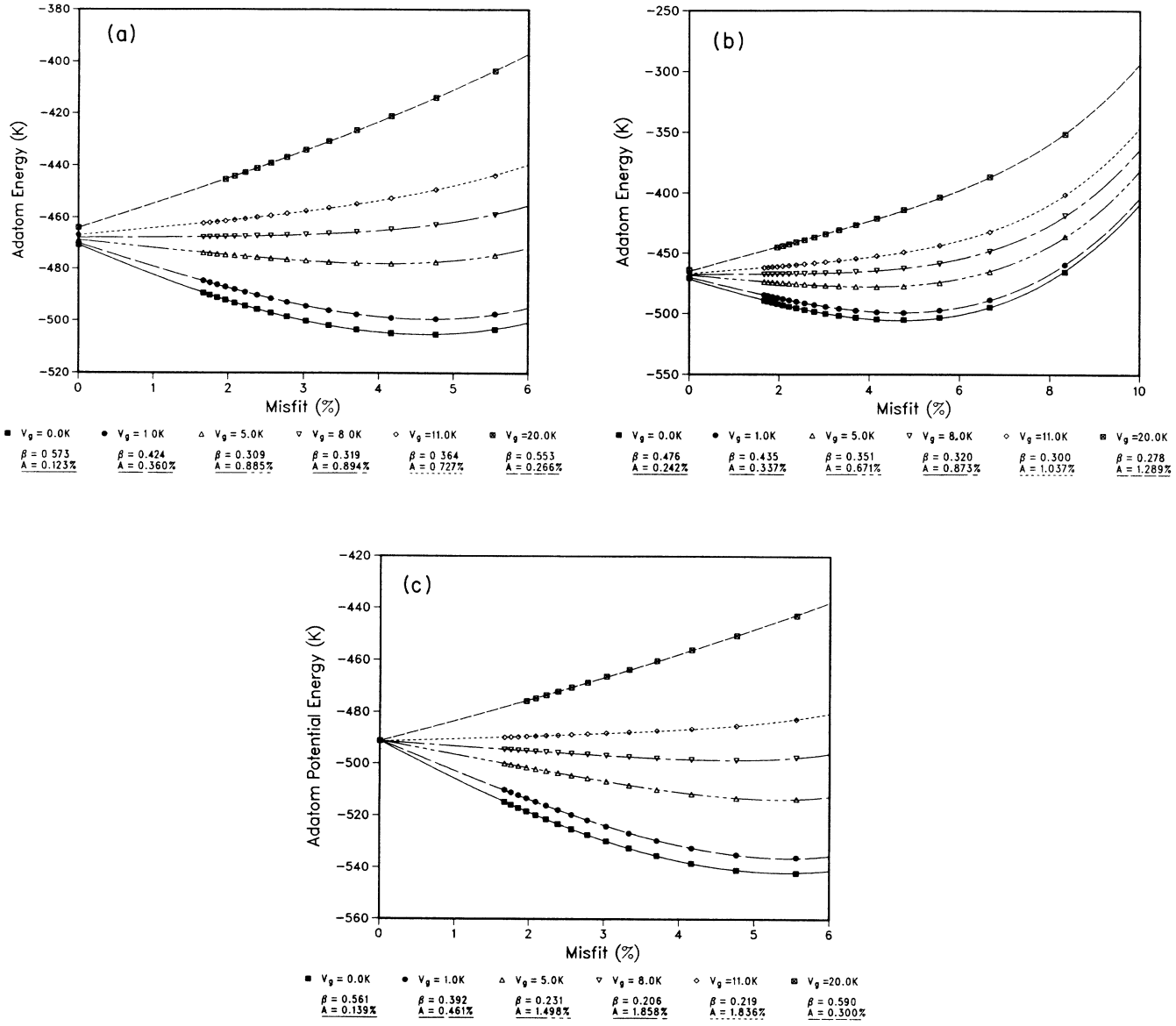

FIG. 7. (a) Free energy per adatom as a function of misfit ε for a variety of substrate corrugations. The curves shown are the best fits of Eq. (20) with the parameters of the fit shown in the legend. (b) As in (a), but with a larger range of misfit values considered for the parametrized fit of Eq. (20). (c) As in (a), but showing only the static potential-energy contribution to the free energy per adatom.

structure, the value of the substrate corrugation will not influence the value of β. The value of β will therefore not be influenced by the broadening of the domain walls with temperature. The experimental observation that the misfit varies with chemical potential as given in Eq. (19) merely reflects the fact that the monolayer has highly interacting domain walls which merge to form a modulated structure at increased misfits. This confirms the prediction of Villain.[31]

At high temperatures, the detailed nature of the domain walls becomes unimportant and the energy associated with the various forms of the domain walls and their fluctuations can be integrated into a few general domain-wall types. Indeed, the various phases and transitions of the monolayer can be well described by a Potts-model calculation which involves domain walls of only two possible orientations.[13,49] At lower temperatures, however, the description of the domain walls must be more accurate if the nature of the monolayer and its transitions are to be modeled accurately. The Potts-model calculation by Caflisch *et al.*[13] does not give the proper location of the commensurate-incommensurate transition. The fluid phase, if present, should occur as the density of the monolayer is increased from a coverage of 1.[32] With changes to the parameters of the Potts-model calculation, the location and nature of the low-temperature transitions can be made to vary significantly.[49] It is expected, therefore, that if the superheavy-wall energy is made slightly more favorable than the heavy-wall energy, the predictions of Potts-model calculations should match the predictions of low-temperature calculations.

V. CONCLUSION

Our theory for the low-temperature behavior of the krypton monolayer on graphite incorporates as accurate a description as is practically possible for the microscopic interactions of the system. The energies of different configurations are obtained with both harmonic and cubic approximations to the adatom-interaction potentials. Where the harmonic approximation reproduces Shiba's theory of orientational epitaxy, the inclusion of the cubic term reveals that the orientational behavior will be temperature dependent.

The dynamic behavior of the incommensurate monolayer is examined, and the entropy contribution to the free energy was found to be small for all misfits considered. The interaction between the domain walls, though slight, is sufficient to reduce the entropy associated with the breathing motion of the domain walls. The zero-point energy of the incommensurate monolayer was found to be significant. Its variation with the misfit of the monolayer is a major influence on how the monolayer varies with the chemical potential. In particular, the contribution of the zero-point energy is such that the substrate corrugation value of 7.4 K calculated by Vidali and Cole[42] is sufficient for the monolayer to have a low-temperature commensurate phase.

From the calculated free energies of the monolayer, the variation of the misfit of the monolayer with the chemical potential was examined. The nearly $\frac{1}{3}$ exponent of Eq. (19) measured for the misfit variation with chemical potential is not a universal value, but is simply a consequence of the crossover between the two limiting configurations of the monolayer. Other similar systems may therefore exhibit rather different exponents.

This work has not addressed the nature of the commensurate-incommensurate phase transition. This aspect of the system will be discussed in a following paper. In particular, a domain-wall fluid may occur in the commensurate limit.[32] A link is also sought with renormalized theories which successfully predict a variety of phases and transitions of the monolayer at higher temperatures.[13]

ACKNOWLEDGMENTS

This work has been funded by the Natural Sciences and Engineering Research Council of Canada. We also acknowledge useful comments from L. Bruch and S. Fain.

[1]R. J. Birgeneau and P. M. Horn, Science **232**, 329 (1986).
[2]J. G. Dash, Physics Today **38**(12), 26 (1985).
[3]R. J. Birgeneau, P. A. Heiney, and J. P. Pelz, Physica **109&110B**, 1785 (1982).
[4]For an extensive review, see E. D. Specht, A. Mak, C. Peters, M. Sutton, R. J. Birgeneau, K. L. d'Amico, D. E. Moncton, S. E. Nagler, and P. M. Horn, Z. Phys. B **69**, 347 (1987).
[5]M. D. Chinn and S. C. Fain, Jr., Phys. Rev. Lett. **39**, 146 (1977).
[6]T. Ceva and C. Marti, J. Phys. (Paris) Lett. **39**, L221 (1978).
[7]P. M. Horn, R. J. Birgeneau, P. Heiney, and E. M. Hammonds, Phys. Rev. Lett. **41**, 961 (1978).
[8]P. W. Stephens, P. A. Heiney, R. J. Birgeneau, and P. M. Horn, Phys. Rev. Lett. **43**, 47 (1979).
[9]S. C. Fain, M. D. Chinn, and R. D. Diehl, Phys. Rev. B **21**, 4170 (1980).
[10]P. S. Schabes-Retchkiman and J. A. Venables, Surf. Sci. **105**, 536 (1981).
[11]P. W. Stephens, P. A. Heiney, R. J. Birgeneau, P. M. Horn, D. E. Moncton, and G. S. Brown, Phys. Rev. B **29**, 3512 (1984).
[12]K. L. d'Amico, D. E. Moncton, E. D. Specht, R. J. Birgeneau, S. E. Nagler, and P. M. Horn, Phys. Rev. Lett. **53**, 2250 (1984).
[13]R. G. Caflisch, A. N. Berker, and M. Kardar, Phys. Rev. B **31**, 4527 (1985).
[14]W. A. Steele, Surf. Sci. **36**, 317 (1973).
[15]L. W. Bruch, Surf. Sci. **125**, 194 (1983).
[16]J. Villain, in *Ordering in Strongly Fluctuating Condensed Matter Systems*, edited by T. Riste (Plenum, New York, 1980), p. 221.
[17]R. J. Gooding, B. Joos, and B. Bergersen, Phys. Rev. B **27**, 7669 (1983).
[18]F. F. Abraham, W. E. Rudge, D. J. Auerbach, and S. W. Koch, Phys. Rev. Lett. **52**, 445 (1984).
[19]H. Shiba, J. Phys. Soc. Jpn. **46**, 1852 (1979).
[20]H. Shiba, J. Phys. Soc. Jpn. **48**, 211 (1980).

[21]J. Villain and M. B. Gordon, Surf. Sci. **125**, 1 (1983).
[22]R. A. Aziz, Mol. Phys. **38**, 177 (1979).
[23]S. Rauber, J. R. Klein, and M. W. Cole, Phys. Rev. B **27**, 1314 (1983).
[24]A. D. McLachlan, Mol. Phys. **7**, 381 (1964).
[25]N. D. Shrimpton, B. Bergersen, and B. Joos, Phys. Rev. B **34**, 7334 (1986).
[26]F. W. de Wette, B. Firey, E. de Rouffignac, and G. P. Alldredge, Phys. Rev. B **28**, 4744 (1983).
[27]K. Kern, P. Zeppenfeld, R. David, and G. Comsa, Phys. Rev. B **35**, 886 (1987).
[28]T. H. Ellis, G. Scoles, and U. Valbusa, Chem. Phys. Lett. **94**, 247 (1983).
[29]K. D. Gibson and S. J. Sibener, Phys. Rev. Lett. **55**, 1514 (1985).
[30]B. Hall, D. L. Mills, and J. E. Black, Phys. Rev. B **32**, 4932 (1985).
[31]J. Villain, Surf. Sci. **97**, 219 (1980).
[32]S. N. Coppersmith, D. S. Fisher, B. I. Halperin, P. A. Lee, and W. F. Brinkman, Phys. Rev. B **25**, 349 (1982).
[33]N. D. Shrimpton, B. Bergersen, and B. Joos, Phys. Rev. B **29**, 6999 (1984).
[34]L. W. Bruch, Surf. Sci. **150**, 503 (1985).
[35]A. D. Novaco, Phys. Rev. B **22**, 1645 (1980).
[36]L. K. Moleko, B. Joos, T. M. Hakim, H. R. Glyde, and S. T. Chui, Phys. Rev. B **34**, 2815 (1986).
[37]D. J. Chadi and M. L. Cohen, Phys. Rev. B **8**, 5747 (1973).
[38]S. L. Cunningham, Phys. Rev. B **10**, 4988 (1974).
[39]J. C. Wheeler, M. G. Prais, and C. Blumstein, Phys. Rev. B **10**, 2429 (1974).
[40]J. C. Wheeler and C. Blumstein, Phys. Rev. B **6**, 4380 (1972).
[41]N. D. Shrimpton, Ph.D. thesis, University of British Columbia, 1987.
[42]G. Vidali and M. W. Cole, Phys. Rev. B **29**, 6736 (1984).
[43]A. D. Novaco and J. P. McTague, Phys. Rev. Lett. **38**, 1286 (1977).
[44]J. Frenkel and T. Kontorowa, Phys. Z. Sowjetunion **13**, 1 (1938); F. C. Frank and J. H. van der Merwe, Proc. R. Soc. London, Ser. A **198**, 205 (1949).
[45]M. B. Gordon and F. Lançon, J. Phys. C **18**, 3929 (1985).
[46]M. Schöbinger and S. W. Koch, Z. Phys. B **53**, 233 (1983).
[47]P. Bak, D. Mukamel, J. Villain, and K. Wentowska, Phys. Rev. B **19**, 1610 (1979); J. A. Venables and P. S. Shabes-Retchkiman, Surf. Sci. **71**, 27 (1978).
[48]F. F. Abraham, S. W. Koch, and W. E. Rudge, Phys. Rev. Lett. **49**, 1830 (1982).
[49]M. Kardar and A. N. Berker, Phys. Rev. Lett. **48**, 1552 (1982).